Diffusion along Small-Angle Grain Boundaries in Silicon*

H. J. QUEISSER, K. HUBNER, AND W. SHOCKLEY
Shockley Transistor, Unit of Clevite Transistor, Palo Alto, California

(Received April 5, 1961)

Diffusion fronts in samples containing grain boundaries are spike shaped. Velocity of spike advance and angle between spike and boundary are measured. The "spike-velocity method" of analysis permits evaluation of two effective widths, W_D and W_0, which describe the diffusion properties of the boundary. This method has been used to analyze data on phosphorus diffusion into boron-doped silicon at 1200°C and 1050°C. It is concluded that an enhanced diffusion current flows along each dislocation of the grain boundary over a cross section less than one Burgers-vector square. The diffusion current density is about 300 000 times that of the bulk. This corresponds to an energy of 1.5 ev by which grain boundary diffusion is favored over the bulk diffusion. This enhancement is believed to be caused by enrichment of phosphorus and also partly by the extra concentration of vacancies near the dislocation cores. Some possible extensions of the studies to include saturation effects at the dislocation cores are discussed.

1. INTRODUCTION

SMALL-ANGLE grain boundaries in silicon afford an unusually excellent means of studying the effect of dislocations upon the diffusion of solute atoms in crystals.

The idea that a small-angle grain boundary is composed of an array of dislocations was introduced independently by Bragg[1] and Burgers.[2] Experimental confirmation in which dislocations were identified with etch pits was offered by Shockley and Read[3] using data of Lacombe[4]; and later, more completely, by Vogel, Pfann, Corey, and Thomas.[5] Further evidence that a grain boundary may be regarded as composed of individual dislocations is furnished by the comparison of the Read-Shockley[6] grain boundary energy formula with experiments.[7] These indicate that the small-angle model certainly applies for angles up to at least 15° (for germanium).[8]

Since the grain boundaries studied here have angles less than 8°, they should give the combined effects of the many dislocations. Such cumulative effects are much easier to observe than the effects of individual dislocations.

Silicon and germanium lend themselves well to such studies because of the possibility of revealing *p-n* junctions by staining. As a consequence, donors may be diffused into uniform *p*-type material and isoconcentration boundaries, where donor density equals acceptor density, are readily shown.[9] This method of studying grain boundary diffusion has been reported for germanium by Karstensen[10,11] and for silicon by Hubner and Shockley.[12] In this article, a more complete discussion of methods of analyzing the data for phosphorus in silicon is presented. The results are interpreted in terms of the diffusion properties of individual dislocations.

Previous work on grain boundary diffusion has included both experiment and analysis.[13] It has shown that diffusion along grain boundaries proceeds much faster than in the bulk. Mathematical analyses have been given by Fisher,[14] LeClaire,[15] and Whipple.[16] Fisher gives an approximate treatment, and it is not easily possible (see Whipple) to estimate its accuracy. Whipple gives an exact treatment which leads to formidable expressions, difficult to compare with experiment.[10]

Previous analyses treated the grain boundary as a sheet with given geometry and a diffusivity assumed *a priori* to be higher than in the bulk. From the physical point of view, there seems to be a lack of attention to the role of accumulations along the grain boundary. The way in which these should enter the theory is discussed in the following sections.

The "spike-velocity" method of analyzing data is used in this study. This method has several advantages over previous methods: (1) It is exact in the range where diffusion currents are linear in the concentrations; (2) it has a relatively simple mathematical form; (3) it is independent of the boundary conditions prevailing at a distance from the isoconcentration line being studied.

The spike-velocity method is applied to data on phosphorus diffusing into silicon at 1200°C and 1050°C.

[1] W. L. Bragg, Proc. Phys. Soc. (London) **52**, 54 (1940).
[2] J. M. Burgers, Proc. Phys. Soc. (London) **52**, 23 (1940).
[3] W. Shockley and W. T. Read, Phys. Rev. **75**, 692 (1949).
[4] P. Lacombe, *Proceedings of the Conference on Strength of Solids, University of Bristol, England, 1948* (The Physical Society, London), p. 91.
[5] F. L. Vogel, W. G. Pfann, H. E. Corey, and E. E. Thomas, Phys. Rev. **90**, 489 (1953).
[6] W. T. Read and W. Shockley, Phys. Rev. **78**, 275 (1950); see also reference 3.
[7] Summary of the experimental results in: S. Amelinckx and W. Dekeyser, in *Solid-State Physics*, edited by F. Seitz and D. Turnbull (Academic Press, Inc., New York, London, 1959), Vol. 8, p. 420.
[8] R. S. Wagner and B. Chalmers, J. Appl. Phys. **31**, 581 (1959).
[9] C. S. Fuller and J. A. Ditzenberger, J. Appl. Phys. **27**, 544 (1956).
[10] F. Karstensen, Z. Naturforsch. **14a**, 1031 (1959).
[11] F. Karstensen, J. Electronics and Control **3**, 305 (1957).
[12] K. Hubner and W. Shockley in *Structure and Properties of Thin Films*, edited by Neugebauer *et al.* (John Wiley & Sons, Inc., New York, 1959), p. 302; Bull. Am. Phys. Soc. **4**, 409 (1959).
[13] A review and compilation of references will be found in the article by S. Amelinckx and W. Dekeyser (reference 7). See also P. Lacombe in *La Diffusion dans les Metaux* (Philips Technical Library, Eindhoven, 1957), p. 23.
[14] J. Fisher, J. Appl. Phys. **22**, 74 (1951).
[15] A. D. LeClaire, Phil. Mag. **42**, 468 (1951).
[16] R. T. P. Whipple, Phil. Mag. **45**, 1225 (1954).

2. BOUNDARY CONDITION ON THE GRAIN BOUNDARY

The mathematical description of the grain boundary diffusion depends on a reasonable mathematical approximation. This approximation will in general be valid for low concentrations (where the effects are linear in concentration) and for diffusion depths which are large compared to the fine structure (dislocation spacing) in the grain boundary. The approximation involves what may be called *proportional disturbances*. A proportional disturbance is one in which the distribution of solute atoms in any small region of the grain boundary is proportional to the concentration in the bulk just outside the boundary. Furthermore, as the concentration of the solute just outside the boundary is changed, the concentration within the boundary varies in the same way from place to place as it would in thermal equilibrium. In other words, the fractional disturbance from a thermal equilibrium distribution is small in a region of extent comparable to the dislocation spacing. (In Appendix A2, we consider a case in which the approximation of proportional disturbances must be modified).

In terms of this assumption, the boundary-value problem may be treated as follows.

For the case of thermal equilibrium the concentration $c(x,y,z)$ has a uniform value c_0 in the bulk. Throughout the volume of Fig. 1, it may be written as

$$c(x,y,z)=c_0 f(x,y,z), \tag{1}$$

where $f(x,y,z)$ is practically unity at a few dislocation spacings away from the grain boundary.

A volume like Fig. 1 contains more solute atoms than an equal volume of perfect crystal because of the presence of the grain boundary. The extra number of solute atoms per unit area of the grain boundary may be written as $c_0 W_0$, where

$$c_0 W_0=\int\int\int c_0[f(x,y,z)-1]dxdydz \Big/ \int\int dydz, \tag{2}$$

where the integrals extend over the volume and the y-z face of Fig. 1. Evidently W_0 is an effective *concentration width* and may be thought of as arising from an effective physical width times a concentration factor. (We shall discuss an estimate of W_0 from the dislocation model in the next section.)

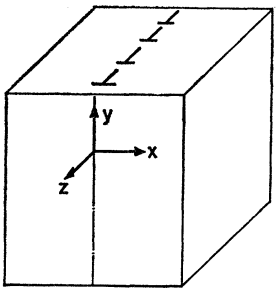

FIG. 1. Coordinate system used for discussing diffusion down a small-angle grain boundary.

Under nonequilibrium conditions, concentration gradients will be present. The diffusion current in the bulk will be $-D\nabla c(x,y,z,t)$, and the equation of continuity is

$$\partial c/\partial t=D\nabla^2 c, \tag{3}$$

where D is the bulk diffusion constant.

In accordance with the proportional disturbance assumption, the bulk concentration just outside the grain boundary will approach the same value $c_b(y,z,t)$ from both sides:

$$\lim_{x\to 0} c(x,y,z,t)=c_b(y,z,t). \tag{4}$$

[The physical reason for this is that the diffusion constant in the x direction in the grain boundary at least equals the bulk diffusion constant. Therefore the grain boundary presents a negligible barrier to diffusion across its plane when $(Dt)^{\frac{1}{2}}$ is large compared to the physical thickness of the grain boundary.]

The diffusion current in the grain boundary adds a total additional flux of solute atoms crossing a $y=$constant plane per unit time per unit length which may be written as

$$F_{b,y}=-DW_{D,y}\partial c_b/\partial y. \tag{5}$$

A similar expression applies to the z direction. (For more general boundaries than Fig. 1, a rotation to principal axes for diffusion currents will be necessary.) $W_{D,y}$ may be thought of as arising from the concentration factor $f(x,y,z)$ times an additional boost factor for a higher diffusion constant within the grain boundary. Its value in terms of contributions from individual dislocations will be discussed below.

Figure 2 shows how the grain-boundary boundary condition results from the principle of continuity. It is drawn to correspond to the diffusion situation encountered experimentally with diffusion proceeding in the $+y$ direction of Fig. 1, and the isoconcentration line in the bulk intersecting at an angle θ with the boundary. The relationship of an isoconcentration line to the x and y components of flux is illustrated. The rate of accumula-

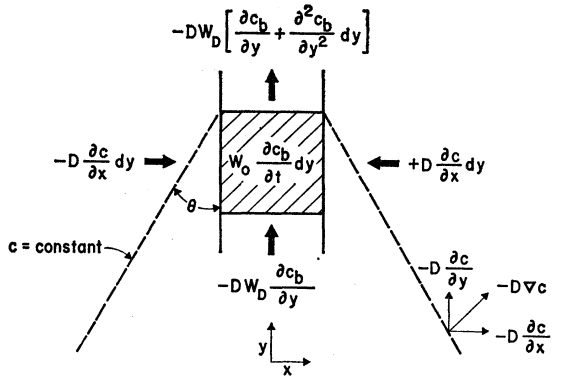

FIG. 2. Illustration of boundary condition, expressed in terms of W_0 and W_D.

tion of solute atoms per unit area of the grain boundary is obtained by adding the fluxes into the element dy of Fig. 2 and dividing by dy. This leads readily to an equation which represents the divergence of flux in the grain boundary plane plus the inward fluxes from the two sides. When a flux in the z direction is present, the divergence of this must be included. This leads to

$$W_0\partial c_b/\partial t = D[(\partial c/\partial x)_+ - (\partial c/\partial x)_-] + DW_{D,y}(\partial^2 c_b/\partial y^2) + DW_{D,z}(\partial^2 c_b/\partial z^2), \quad (6)$$

where the derivatives in respect to x are limits as $x \rightarrow 0$ from the $x>0$ and $x<0$ sides of the grain boundary.[17]

This equation is mathematically equivalent to previously used boundary conditions.[14–16] However, the interpretation of the coefficients given here is different.

3. ORIGIN OF W_0 AND W_D FOR A DISLOCATION MODEL OF A SMALL-ANGLE GRAIN BOUNDARY

The case of interest in this study is that of a tilt boundary with edge dislocations running parallel to the y axis of Fig. 1. We shall estimate values of W_0 and $W_D \equiv W_{D,y}$ on the Cottrell[18,19] model of atmospheres around dislocations.

In accordance with the dislocation model of grain boundaries, the spacing S of edge dislocations is, for the simplest case and for small angles

$$S = b/\phi, \quad (7)$$

where ϕ is the tilt angle and b the Burgers vector. For grain boundaries of more complex geometry, there may be several types of dislocations present. Formulas will be found in the literature.[6,20] (For the case of Sec. 5 below, a factor of $\sqrt{2}$ occurs.)

Edge dislocations are surrounded by a region of compression and dilatation. Consider an impurity atom with a radius $r_i = r_{Si}(1+\epsilon_i)$, where r_{Si} is the silicon atom radius. At a point with the polar coordinates r, α from the dislocation core, that atom has a potential energy U, given by Cottrell's formula[18,19]:

$$U = (A/r)\sin\alpha. \quad (8)$$

This energy depends only upon $|\epsilon_i|$. The negative sign for ϵ_i indicates that the compression side of the dislocation is occupied, the positive sign–dilation side. The maximum binding energy, U_i, is approximately A_i/r_0, where r_0 is the distance from core to edge of the extra half-plane and is given by

$$U_i = A_i/r_0 = 3|\epsilon_i| V\mu b/\pi r_0 = 7.7(|\epsilon_i| b/r_0) \text{ ev}, \quad (9)$$

where μ is the rigidity modulus (6×10^{11} dynes/cm^2 $=3.7\times10^{23}$ ev/cm^3) for silicon, and $V=2\times10^{-23}$ cm^3 is the volume per silicon atom. For the case where $\exp(U_i/kT)$ is large, the atmosphere is concentrated essentially on the single column or pair of columns of sites nearest the dislocation and the extra impurities per unit length are approximately equal in number to those contained in a column of area $b^2\exp(U_i/kT)$ of bulk material.

A tilt boundary of tilt angle ϕ containing ϕ/b dislocations per unit length in the z direction of Fig. 1 thus contains extra impurities equal to the number in a slab of bulk material of thickness W_0:

$$W_0 = [b^2\exp(U_i/kT)]/S. \quad (10)$$

Vacancies are also assumed to be concentrated in the same region by a factor $\exp(U_v/kT)$. U_v probably cannot be computed by considering a vacancy to be an atom with an effective ϵ_v. There seems to be very little information on the thermal equilibrium distribution of vacancies near a dislocation.[21] It seems probable that large and small stress fields will have quite different effects. In weak stress fields a vacancy probably has an energy given by the Cottrell potential, Eq. (8), with an effective negative ϵ_v corresponding to an undersized solute atom. Near the core of the dislocation the strains of both compression and extension exceed the linear range substantially. It would apparently reduce the total energy of the system to move a vacancy from a point far from the dislocation to either the most highly compressed or most dilated rows closest to the core. Thus we would expect that vacancies would tend to be more abundant near the core than in the bulk and that this would be true for both the tension and compression sides of the dislocation.

If the vacancy mechanism controls diffusion down the dislocation core, then it will be enhanced compared to the bulk by both the factor $\exp(U_i/kT)$ and by $\exp(U_v/kT)$. In addition, the potential energy barrier for jump into a vacancy may be lowered by U_j because of the extra flexibility associated with the dilatation near the dislocation core.

According to the preceding reasoning, each dislocation contributes a diffusion current equivalent to a column of bulk material of area $b^2\exp[(U_i+U_v+U_j)/kT]$.

Again introducing the number of dislocations per unit length in the z direction of Fig. 1, we obtain

$$W_D = b\phi\exp(U_D/kT), \quad (11)$$

[17] This equation and its interpretation was published by W. Shockley, C. S. Roberts, and J. Hoerni, Bull. Am. Phys. Soc. **2**, 202 (1957).

[18] A. H. Cottrell, *Proceedings of the Conference on Strength of Solids, University of Bristol, England, 1948* (The Physical Society, London), p. 30; also *Dislocations and Plastic Flow in Crystals* (Clarendon Press, Oxford, England, 1953), p. 56.

[19] Equation (8) incorporates a modification suggested by B. A. Bilby, Proc. Phys. Soc. (London) **A63**, 191 (1950). See also *Dislocations and Plastic Flow in Crystals* (reference 18), p. 57.

[20] W. T. Read, *Dislocations in Crystals* (McGraw-Hill Book Company, Inc., New York, 1953), p. 173.

[21] A viewpoint similar to that presented here was expressed by A. H. Cottrell in *Point Defects and the Mechanical Properties of Metals and Alloys at Low Temperatures* (Institute of Metals, London, 1958), p. 22. However, there appear to be no quantitative estimates of the effects such as might be required to evaluate U_v in Eq. (12). See also *Dislocations and Plastic Flow in Crystals* (reference 18), p. 175.

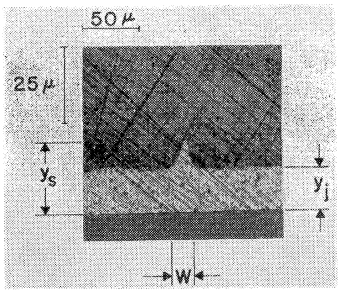

FIG. 3. Photograph of a beveled and stained p-n junction showing the diffusion front at the grain boundary.

where U_D is defined as

$$U_D \equiv U_i + U_v + U_j. \tag{12}$$

In the following section the spike velocity method of deducing W_0 and W_D from experimentally measured quantities is discussed. Actual data are analyzed in subsequent sections.

4. THE SPIKE-VELOCITY METHOD OF ANALYSIS

The grain boundary equation (6), together with the bulk diffusion equation, constitutes a set of partial differential equations which lead uniquely to a concentration $c(x,y,z,t)$ once the initial and boundary conditions are specified. The solutions are very involved,[16] since in addition to the space variables x,y,z they include three quantities having the dimensions of length: $(Dt)^{\frac{1}{2}}$, W_D, W_0. Furthermore, if during part of the diffusion the concentration exceeds the linear range, or the surface boundary conditions change, the solutions may be invalid.

The spike-velocity method makes use of the fact that an isoconcentration line,

$$c(x,y,t) = c_0, \tag{13}$$

has an intercept on the grain boundary with an included angle 2θ. (See Figs. 3, 4, and 6.) The spike advances with a velocity

$$v = dy/dt. \tag{14}$$

As is shown in Appendix A1,

$$(v \tan\theta)^{-1} = (W_D \sin^2\theta - W_0)/2D. \tag{15}$$

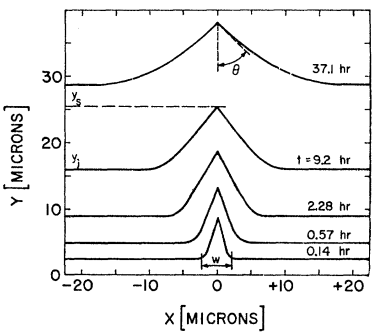

FIG. 4. p-n junction profiles or isoconcentration lines for phosphorus diffusion at 1200°C from measurements on photomicrographs of stained, beveled junctions.

This equation, which we refer to as the *spike-velocity equation*, is the basis of our analysis. In principle it permits the determination of the constants W_D and W_0 from measurements of v, θ, and D.

An advantage of using the spike-velocity method is that concentrations may be present which are so high that the linear approximation does not apply. Nevertheless, if the concentration contour being observed lies in the linear range, the equation is valid. A disadvantage of the equation is that it requires taking a time derivative. This difficulty may be overcome by fitting the data for $y(t)$ at the spike by a simple analytical expression and then obtaining v by differentiation. An important advantage is, of course, the simplicity of the expression.

5. EXPERIMENT AT 1200°C

A bi-crystal was prepared having a [100] growth axis. The two grains were rotated about this axis by $7.5 \pm 0.25°$ in respect to each other and joined, approximately symmetrically, across a (010) plane. The dislocation array in the grain boundary is thought to consist of alternating $\frac{1}{2}a[011]$ and $\frac{1}{2}a[01\bar{1}]$ Burgers vector dislocations running on [100] lines.[8,22] For silicon, the lattice constant $a = 5.42$ A and the Burgers vector has the magnitude

$$b = a/\sqrt{2} = 5.42/\sqrt{2} = 3.83 \text{ A}. \tag{16}$$

The spacing S between dislocations for this geometry is for small angles

$$S = b/\phi\sqrt{2} = 21 \text{ A}, \tag{17}$$

the spacing between similar dislocations being twice as much.

The crystal as grown contained boron and had a resistivity of 0.125 ohm cm corresponding to an acceptor density of $N_a = 1.2 \times 10^{18}$ cm^{-3}.

A slice was cut perpendicular to the growth axis of the bi-crystal. It was lapped and mechanically polished. A chemical etch was avoided, since it would have etched the surface preferentially at the grain boundary.

Phosphorus was deposited onto the sample by heating for 0.5 hr at 900°C in the presence of a P_2O_5 source. The subsequent diffusions were performed at 1200°C in an oxygen ambient without source. All data were measured on the same slice. The angle θ and the junction depths in the bulk and at the grain boundary were obtained with beveling and staining techniques.[9] Figure 3 shows a photograph, and Fig. 4 the diffusion profiles as plotted from measurements of such photographs. Table I gives the numerical values of the experimental data, together with figures from an analytic expression used to smooth the data. For the penetration of the spike this expression was

$$y_s = 14.5 t^{0.265} \text{ microns}, \tag{18}$$

for t in hours. The velocity v is obtained by differentiat-

[22] W. G. Pfann and F. L. Vogel, Acta Met. 7, 377 (1957).

TABLE I. Diffusion of phosphorus in silicon at 1200°C. (Units: microns and hours.)

t	Total diffusion time	0.143	0.57	2.28	9.2	37.1
y_j	Junction depth					
	measured	2.4	4.8	8.9	15.8	28.6
	smoothed	2.5	4.65	8.7	16.0	29.0
y_s	Spike depth					
	measured	8.75	13.2	18.8	25.4	38.1
	smoothed	8.6	12.5	18.0	26.1	37.0
W	Spike width	4.4	8.4	12.6	20	36
$\tan\theta$		0.18–0.35	0.25–0.50	0.45–0.61	0.75±0.07	1.36±0.13
$\sin^2\theta$		0.03–0.11	0.06–0.20	0.17–0.27	0.36±0.04	0.65±0.09
v		16	6.1	2.2	0.73	0.27
$(v\tan\theta)^{-1}$		0.18–0.36	0.33–0.67	0.75–1.0	1.8 ±0.2	2.7 ±0.3

ing and is estimated to be accurate to better than ±10%. The calculated bulk junction depths are given by

$$y_j=2L[\ln(L_0/L)]^{\frac{1}{2}}, \tag{19}$$

corresponding to rewriting the Gaussian distribution, where $L=(Dt)^{\frac{1}{2}}$ for $D=1.98\ \mu^2$/hr. This diffusion coefficient is higher by a factor of 2 than the quoted value.[9] $L_0=140\ \mu$, corresponding to an initial deposit Q of

$$Q=N_aL_0\pi^{\frac{1}{2}}=1.2\times10^{18}\times1.4\times10^{-2}\times1.78$$
$$=3.0\times10^{16}\text{ phosphorus atoms/cm}^2. \tag{20}$$

The value of $\tan\theta$ is difficult to determine for small values of time, and $\tan\theta$ has been estimated as

$$\tan\theta=(0.75\pm0.25)(W/2)/(y_s-y_j) \tag{21}$$

for the first two measurements. The range of the plot of $(v\tan\theta)^{-1}$ is indicated by an arc in Fig. 5 and the best estimate by a dot. The errors of the two larger times are estimated on the basis of 10% errors in $(v\tan\theta)^{-1}$ and $\sin^2\theta$.

The plot of $(v\tan\theta)^{-1}$ vs $\sin^2\theta$ in Fig. 5 shows that the predicted relationship, Eq. (15), holds and yields $W_D=18\ \mu$ at 1200°C. W_0 is too small to be measured.

[It should be noted that values of W_D are affected by thermal expansion. If the isoconcentration contours could be observed at 1200°C, all of the dimensions of Fig. 4 would be scaled up by the thermal expansion coefficient of silicon. (This is a factor of about 1.004.) The same comments apply to D. The unit of length is thus, in effect, an equivalent room temperature micron which becomes about 1.004 μ at 1200°C.]

6. EXPERIMENT AT 1050°C

A similar experiment was carried out at 1050°C. The specimen had a resistivity of 0.34 ohm cm. This resistivity corresponds to $N_a=1.7\times10^{17}$ boron atoms/cm³.

The grain boundary was isoaxial with a [100] growth axis and had an angle of misfit of 4.5±0.25°. It was, however, nonsymmetrical. The boundary ran almost parallel to the $(01\bar{1})$ planes in one of the grains. The dislocation array is thought to consist essentially of dislocations with a Burgers vector $b_1=\frac{1}{2}a[01\bar{1}]$ along a [100] line. For this nonsymmetrical boundary, additional dislocations with a Burgers vector $b_2=\frac{1}{2}a[011]$ must be assumed. Their number, however, amounts to less than 1% of the total because of the small misfit angle of the grain boundary. Thus no great error is introduced by treating this grain boundary as symmetrical. The dislocation spacing then is

$$S=b/\phi=55\text{ A}. \tag{22}$$

As in the experiment discussed above, the diffusion of the phosphorus impurities was performed on a polished slice which was cut perpendicular to the growth axis. The diffusion profiles obtained are shown in Fig. 6. The analytical expression used for smoothing the data of the spike penetration depth is

$$y_s=11.5t^{0.125}. \tag{23}$$

Differentiation of Eq. (23) yields v.

The data for the junction depth y_j in the undisturbed material may be fitted with the following expression:

$$y_j=2.2t^{0.376}. \tag{24}$$

Measured and smoothed data are given in Table II.

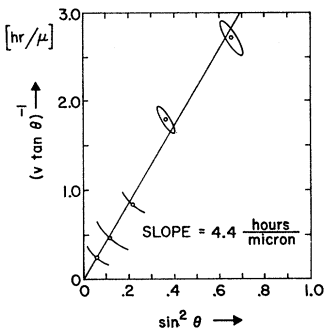

FIG. 5. Plot of experimental data at 1200°C in accordance with the spike-velocity equation (15).

TABLE II. Diffusion of phosphorus in silicon at 1050°C.

t	Total diffusion time [hr]	0.5[a]	1.0	2.0	4.0	16	80.3	133
y_j	Junction depth, measured [μ]	1.8	2.3	2.9	3.6	6.0	10.8	12.9
	smoothed	1.7	2.2	2.8	3.6	6.0	11.0	13.4
y_s	Spike depth, measured [μ]	10.5	11.4	12.1	12.7	16.2	21.0	25.8
	smoothed	10.6	11.6	12.7	13.8	16.4	20.0	21.5
W	Spike width [μ]	2.8	4.1	4.8	5.4	8.2	11.2	13.6
$\tan\theta$		0.147	0.185	0.230	0.290	0.425	0.750	0.900
$\sin^2\theta$	(±10%)	0.0213	0.0335	0.0502	0.0778	0.153	0.360	0.447
v	Velocity [μ/hr]	2.6	1.4	0.8	0.4	0.13	0.03	0.02
$(v\tan\theta)^{-1}$	[hr/μ] (±10%)	2.6	3.8	5.5	8.0	18.4	42.5	55.6
ρ	Sheet resistance [ohms/square]	2.90	2.22	1.77	1.31	0.91	0.82	1.00
Q	Predeposit strength [10^{16} atoms/cm^2]	4.4	3.8	4.8	6.5	9.7	10.4	8.2
D	Diffusion coefficient [μ^2/hr]	0.232	0.174	0.145	0.114	0.070	0.045	0.042

[a] Diffusion with P_2O_5 source; all others without source.

The method for determination of the diffusion coefficient D, applied to the former experiment, cannot be used here. The penetrations y_j cannot be described with a constant value of D. Evidence of this may be deduced from Eq. (24). The exponent should be close to 0.5, if the diffusion equation with constant D were valid.

Therefore, the analysis of D was done with a method similar to the one used by Fuller and Ditzenberger.[9] The measured values of the junction depths were used together with the sheet resistance data, given in Table I, for the calculation of D. The carrier mobility data used in our analysis are those of Backenstoss.[23]

The diffusion conditions of this experiment differed in some respects from the above-mentioned run at 1200°C. The initial deposit (predeposit) of phosphorus in the experiment was done at 1050°C, as was the diffusion. This relatively high predeposit temperature resulted in a junction penetration y_j which is not negligible as it was for the 900°C predeposit, 1200°C diffusion experiment. The predeposit time of 0.5 hr must therefore be added to the total diffusion time.

It is assumed that the predeposit results in a complementary error function distribution. This deposit then spreads out upon further heating according to a Gaussian distribution. Using these assumptions one can calculate the total amount Q of phosphorus atoms in the silicon. From the sheet resistance and junction depth measurements a value for Q is found for each diffusion time t. These values of Q are given in Table II. The values spread around an average of 7×10^{16} atoms/cm^2; the shallow diffusions seem to give consistently lower values. This discrepancy will be discussed below in connection with similar anomalies in the diffusion coefficient. It is believed that the spread in the Q values is small enough to justify this method of analysis.

The analysis which gives the Q values also leads to the diffusion coefficients. They are given in the last row of Table II. It is observed that D drops from a value of 0.23 μ^2/hr for the shallow penetrations to an apparent asymptotic value of 0.04 μ^2/hr for the deeper penetrations. The value reported in the literature,[9] obtained under different conditions, is 0.036 μ^2/hr.

Similar observations of such "abnormally" high diffusion coefficients close to the surface have frequently been made in this laboratory.[24,25] The mechanism which is responsible for the enhanced diffusion close to the surface is thus far unknown. It may possibly be linked to another phenomenon which was recently discovered by Tannenbaum.[26] She investigated the diffusion profiles of very shallow junctions by means of anodic oxidation and radioactive tracer techniques. It was found that an appreciable amount of the diffused phosphorus, as traced by its radioactivity, could not be detected through sheet resistance measurements. This means that close to the silicon surface there are phosphorus atoms which are not acting as donors. The same effect

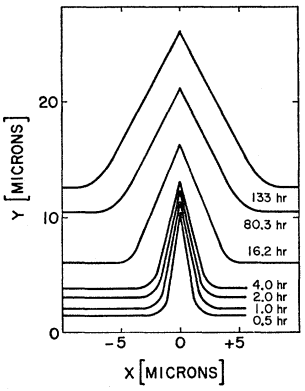

FIG. 6. p-n junction profiles or isoconcentration lines for phosphorus diffusion at 1050°C from measurements on photomicrographs of stained, beveled junctions.

[23] G. Backenstoss, Bell System Tech. J. **37**, 699 (1958).

[24] A. Goetzberger and W. Shockley, Bull. Am. Phys. Soc. **4**, 455 (1959).

[25] B. McDonald and F. C. Collins, Bull. Am. Phys. Soc. **6**, 106 (1961).

[26] E. Tannenbaum (unpublished). Similar experiments are described in reference 25, which essentially confirm Tannenbaum's results.

may be responsible for the apparent depression of the Q values for shallow diffusions reported here. It might be that upon deeper diffusions more phosphorus atoms become active as donors. This would lead to an increase of Q values, which are determined from electrical measurements alone.

It is believed that the spike-velocity method is applicable even with the discussed diffusion anomalies. Figure 7 gives a plot of $(v\tan\theta)^{-1}$ vs $\sin^2\theta$, using the data of Table II. The straight line indicates that Eq. (15) is fulfilled. Again W_0 is too small to be measured and will be neglected. W_D is given by the slope of the line of Fig. 7, multiplied by $2D$. It follows that a constant value of W_D will result only if D is assumed to be constant.

It is felt that the assumption of a constant D—and therefore a constant W_D—can be made on the basis of the following considerations: (1) The smallest spike penetration y_s is about 10 μ. (2) It is a special feature of the spike-velocity method that only the conditions at the tip of the spike are taken into account. (This was explained in Sec. 2 of this paper; see also Fig. 2.) The diffusion coefficient D in the equations is the one at the depth of the spike tip. (3) At depths greater than 10 μ the diffusion behavior appears to be "normal," yielding the literature value of D, and probably no more discrepancies in Q.

For the evaluation of W_D the value $D=0.04$ μ^2/hr is used. From Eq. (15), $W_D=10$ μ for the experiment at 1050°C.

Some features of the diffusion profiles that were not reliably reproducible have been omitted. Many diffusion front profiles, as in Figs. 4 and 6, especially those taken after longer diffusion times, showed a marked reduction of the bulk junction depth at the intersection of bulk and spike junction. This effect has also been observed by Karstensen.[27]

There are two possible explanations for this behavior. It may be caused by diffusion into a nonuniformly doped material, with higher doping at and around the grain boundary. This effect will be visible only if the gradient of the indiffusing phosphorus has become low enough. Or, reversal of the diffusion flux toward the grain boundary because of depletion there, due to the fast downward diffusion, might cause this effect.

If this reasoning were correct, the effect should be reproducible. Present techniques, especially the staining, are not reliable enough to furnish valid conclusions. It is hoped that current investigations will permit more definite statements.

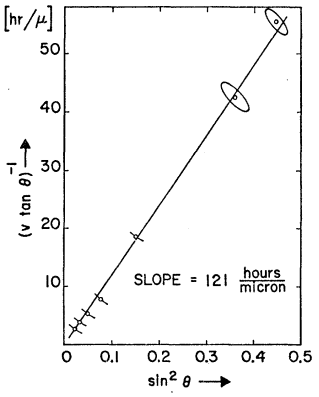

FIG. 7. Plot of experimental data at 1050°C in accordance with the spike-velocity equation (15).

7. INTERPRETATION AND DISCUSSION

Despite the use of differently oriented grain boundaries and different temperatures, all of the experiments may be discussed on the same basis. This is clear when the diffusion properties of the grain boundaries are reduced to those of the single dislocations. One common activation or "favoring" energy U_D, as defined by Eq. (12), describes both diffusion runs.

The grain boundary diffusion current per dislocation is larger than the diffusion current for a column of area b^2 by the factor SW_D/b^2 or 3.7×10^5 and 2.5×10^5 at 1050 and 1200°C, respectively. [$S=55$ A at 1050°C from Eq. (22), and 21 A at 1200°C from Eq. (17); $b^2=14.7\times10^{-16}$ cm^2.]

The corresponding activation energy values are:

$$U_D=kT\ln(SW_D/b^2)=1.5 \text{ ev at } 1050°\text{C}$$
$$=1.6 \text{ ev at } 1200°\text{C}. \quad (25)$$

These two values agree reasonably well. We shall take $U_D=1.5$ ev for comparison with calculations to be discussed later in this chapter.

The central problem in interpreting diffusion down dislocations is that of constructing a model for the core of the dislocation. Conversely, information on diffusion down dislocations may lead to unambiguous identification of the core structure.

Dislocations in the diamond structure are more complex than those in simple lattices, and in general may be of two broad types—those with broken or dangling bonds, and those in which all the valence electrons are paired in electron pair bonds with some distortion of bond length and angles. Experimental evidence against the dangling-bond model in its simplest form is lack of observation of both spin resonance[28] and strong conduction effects.[29]

Hornstra[30] has shown that an edge dislocation with a

[27] F. Karstensen, Z. Naturforsch. **14a**, 1038a (1959), Figures 5, 10a, 10a'.

[28] W. T. Read and G. L. Pearson, *Report of Bristol Conference on Defects in Crystalline Solids*, July, 1954 (The Physical Society, London, 1955), p. 144.

[29] The effect of the grain boundaries studied in this paper upon reverse currents in *n-p* junctions was investigated in this laboratory. (Adolf Goetzberger, paper Q4, International Conference on Semiconductor Physics, Prague, 1960). The fact that "hard" reverse current-voltage characteristics may be obtained indicates that conductivity along grain boundaries is at least five orders of magnitude smaller than would be expected from one-dimensional energy bands due to dangling bonds.

[30] J. Hornstra, J. Phys. Chem. Solids **5**, 129 (1958).

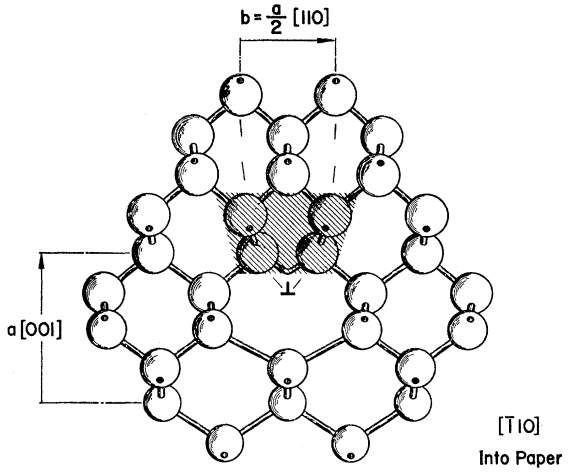

FIG. 8. Atomic positions in the (110) plane due to an edge dislocation with Burgers vector $\frac{1}{2}a[\bar{1}10]$ are shown according to Hornstra's model[27] in which all electrons are paired. The dashed lines indicate the part of the drawing which may be associated with the extra half-plane of the edge dislocation. If the material between the dashed lines were removed and the resulting half-atoms joined, a perfect structure would result. The figure shows atoms in two planes representing one period in the $[\bar{1}10]$ direction. The locations of bonds from the missing plane of atoms above the plane of the figure are indicated.

$\frac{1}{2}a[\bar{1}10]$ Burgers vector and a $[\bar{1}\bar{1}0]$ axis can be formed with all electrons paired as shown in Fig. 8. The bond angles for the two atoms immediately above the dislocation symbol are badly distorted. A screw dislocation can close its bonds with less distortion.

The axis of the dislocation of Fig. 8 can be rotated to $[\bar{1}00]$ or to $[010]$ by shifting the pattern of Fig. 8 sidewise as one proceeds into the paper from one $(\bar{1}10)$ plane to the next $(\bar{1}10)$ plane. Such dislocations can be combined to form grain boundaries of the type we have investigated. We shall not attempt here to select a best model for the dislocation structure of the grain boundary studied, but will use Fig. 8 to illustrate the general features involved.

The Cottrell energy U_i of Eq. (9) is proportional to the ratio of Burgers vector b to radius r_0 from the axis of the dislocation. From Fig. 8, this ratio is seen to be as large as 2 or 3 for atoms just above the dislocation symbol.

The value of ϵ_i for an ionized phosphorus donor,

$$\epsilon(P^+)=[r(P^+)-r(Si)]/r(Si), \tag{26}$$

needed for Eq. (8) may be estimated from data on the lattice constant of silicon-phosphorus alloys[31] and Vegard's law.[32] This leads to $\epsilon(P^+)=-0.055$. An estimate based on tetrahedral radii with an allowance for the fact that the phosphorus is ionized[33] leads to $\epsilon(P^+)=-0.09$ as follows: $r(Si)=1.17$ A, $r(P)=1.10$ A, and $r(P)-r(P^+)=0.02$ A.

Taking as an average estimate $\epsilon(P^+)=-0.07$ and $b/r_0=2$, we obtain from Eq. (9) the binding energy of P^+:

$$U(P^+)=7.7(2\times 0.07)=1.1 \text{ ev}. \tag{27}$$

For $b/r_0=3$, the value of $U(P^+)$ would be as large as the experimental estimate of 1.5 ev for U_D. At 1200°C, $U(P^+)=1.1$ ev leads to

$$\exp[U(P^+)/kT]=\exp 8.7\approx 6000. \tag{28}$$

The value of U for the next nearest position to the core will be twice as small so that this position will be less important by a factor of about 80. Thus, for a binding energy of 1.1 ev, or even for 0.5 ev, practically all of the contribution to W_0 and also to W_D will come from the columns of sites closest to the core of the dislocation.

With Eq. (28) and the values from Eq. (25), we can estimate W_0 for 1200°C from Eq. (10).

$$W_0=(b^2/S)\exp 8.7=0.7\times 10^{-8}\times 6\times 10^3 = 4\times 10^{-5} \text{ cm}. \tag{29}$$

W_0 could not be determined from the experiments through the intercepts on the $(v\tan\theta)^{-1}$ axes of Figs. 5 and 7, because these intercepts were too small. With Eq. (29) they may be calculated. Taking the case at 1200°C as an example, with Eq. (15) the expected intercept on the $(v\tan\theta)^{-1}$ axis of Fig. 5 may be calculated as

$$W_0/2D=0.4/4=0.1 \text{ hr}/\mu. \tag{30}$$

This falls well within the accuracy of the measurements. The same holds for the experiment at 1050°C.

The value of U_D is more difficult to determine because it involves, besides U_i, the unknown quantities U_v and U_j [see Eq. (12)]. If all of the enhanced diffusion arises from the $U(P^+)=U_i$ term in U_D, then it follows that pronounced variations of W_D with concentration should occur. This conclusion follows from the fact that the isoconcentration line studied at 1200°C corresponds to $N_d=N_a=1.2\times 10^{18}$ cm^{-3}. Since the density of silicon atoms is 5×10^{22} cm^{-3}, the fraction of sites in the bulk occupied by phosphorus is 1 in 40 000. For this case the upper limit of $\exp(U_D/kT)$ that could arise from concentration alone could not be as high as 40 000, for, if it were, the sites would be saturated and they could no longer contribute so greatly to the diffusion current in the grain boundary.

The preceding considerations suggest that one experimental approach to finding out about the cores of the dislocations is to investigate saturation effects on W_D. In an Appendix we show that, at high concentrations,

$$W_D(c_b)=W_D(0)/[1+c_b\exp(U_i/kT)]^2. \tag{31}$$

where c_b is the atomic fraction of impurity in the bulk near the grain boundary.

It is evident that in the saturation range, strong interference between several types of impurities may occur.

[31] G. L. Pearson and J. J. Bardeen, Phys. Rev. **75**, 865 (1949).
[32] L. Vegard, Z. Physik **5**, 17 (1921); Z. Krist. **67**, 239 (1928).
[33] L. Pauling, *The Nature of the Chemical Bonds* (Cornell University Press, Ithaca, London, Oxford, 1948), p. 169.

For example, the values of ϵ(boron) estimated from lattice constants of boron-silicon alloys[34] is about four times larger than for phosphorus:

$$\epsilon(\text{boron}) = -0.27. \tag{32}$$

This might be expected to lead to near saturation of the core sites by boron. If the dislocation has two adjacent equivalent core sites, as represented in Fig. 8, there should be a strong tendency for pairing of boron and phorphorus ions on them.

It is difficult to reach conclusions about the change in ease of jumping U_j discussed in Sec. 3. This is evidently highly dependent on core structure.

The value of U_i, and hence of W_D, should be greatly enhanced by large mismatch of atomic size. For the acceptors In and Tl and the donors Sb and Bi, the values of ϵ are three or four times larger than for phosphorus. They should lend themselves to a study of saturation effects.

The electrical effects of donors or acceptors bound to the core or close to the dislocations offer an interesting means of studying the phenomena involved. At least two related types of investigation are possible. Conduction of boundaries of one conductivity type in material of another type can be studied. The effect of the charge on the boundary in affecting avalanche multiplication offers another approach.

The investigations reported in this article emphasize the effects produced by donors and acceptors whose distributions have been affected by dislocations. It should be noted that a number of electrical effects[35] have been studied for both large and small angle grain boundaries, particularly in germanium.[36–40] In germanium, grain boundaries tend to be p-type[36] and dislocations act as if their cores have a negative charge with a multiplicity of states which are effective in producing recombination.[37,38] Allen[41] pointed out that the electron energy levels at edge dislocations in germanium will be modified by the presence of impurity atmospheres. The results obtained in the present work suggest that the charge on the dislocation core may be highly dependent upon the nature of the impurity present, at least at higher levels of bulk concentration. There may also be a dependence on the rate of quenching from high temperatures. Until experiments intended to reveal such effects are carried out, it seems improbable that the electrical properties of dislocations can be interpreted reliably in terms of atomic configurations.

[34] F. H. Horn, Phys. Rev. **97**, 1521 (1955).
[35] For a review, see: W. Bardsley, *Progress in Semiconductors* (John Wiley & Sons, Inc., New York, 1960), Vol. 4, p. 157.
[36] G. L. Pearson, Phys. Rev. **76**, 459 (1949).
[37] G. L. Pearson, W. T. Read, and F. J. Morin, Phys. Rev. **93**, 666 (1954).
[38] W. T. Read, Phil. Mag. **45**, 775 and 1119 (1954). F. L. Vogel, W. T. Read, and L. C. Lovell, Phys. Rev. **94**, 1791 (1954).
[39] H. F. Mataré *et al.*, Phys. Rev. **98**, 1179 (1955). H. F. Mataré, Proc. Inst. Elec. Engrs. (London), **B106**, Suppl. 15, 293 (1959), with additional references given.
[40] R. K. Mueller, J. Appl. Phys. **30**, 546 and 1004 (1959).
[41] J. W. Allen, J. Electronics **1**, 580 (1956).

ACKNOWLEDGMENTS

It is a pleasure to acknowledge the assistance of R. Finch in the experimental work, and Dr. V. Macres, of Stanford University, who kindly carried out the x-ray orientation measurements.

APPENDIX A1. DERIVATION OF THE SPIKE-VELOCITY EQUATION

We assume, in keeping with the experimental observation, that the spike advances along the y axis at a rate v. The concentration is constant along a line of the form

$$u = x\cos\theta + y\sin\theta, \quad x>0 \tag{A1.1}$$

as shown in Fig. 2. Near this line, the concentration is taken as a function $c(u,t)$ of u and t.

The spike-velocity equation results from the physical principle of continuity and the proportional disturbance postulate. In particular we require that $\partial c/\partial t$, the rate of change of concentration just outside the boundary, has the same value when calculated from the diffusion equation for the bulk and the boundary condition, Eq. (6). These two rates are expressed in terms of derivatives of c in respect to u as follows:

$$\partial c/\partial t = D\nabla^2 c = D\partial^2 c/\partial u^2, \tag{A1.2}$$

$$\partial c/\partial t = D[W_D(\partial^2 c_b/\partial y^2) + 2(\partial c/\partial x)]/W_0,$$
$$= D[W_D(\partial^2 c/\partial u^2)\sin^2\theta + 2(\partial c/\partial u)\cos\theta]/W_0. \tag{A1.3}$$

The next step is to eliminate the derivative of $\partial^2 c/\partial u^2$ by first introducing the spike velocity v by the equation

$$\partial c/\partial t = -v\partial c/\partial y = -v(\partial c/\partial u)\sin\theta, \tag{A1.4}$$

and substituting this in Eq. (A1.2) to obtain

$$\partial^2 c/\partial u^2 = (\partial c/\partial t)/D = -v\sin\theta(\partial c/\partial u)/D. \tag{A1.5}$$

Inserting (A1.5) into (A1.3) to eliminate $\partial^2 c/\partial u^2$ leads to

$$-v\sin\theta\partial c/\partial u$$
$$= [(-W_D v\sin^3\theta) + 2D\cos\theta](\partial c/\partial u)/W_0. \tag{A1.6}$$

Multiplying this equation by $W_0/2Dv\sin\theta(\partial c/\partial u)$ leads to

$$-W_0/2D = (-W_D\sin^2\theta/2D) + (v\tan\theta)^{-1}, \tag{A1.7}$$

which is easily rearranged to give the spike-velocity equation (15).

APPENDIX A2. SATURATION EFFECTS ON THE DISLOCATION CORE

We shall here estimate the diffusion current down the central column at the core of the dislocation for the case of high concentrations. We shall assume that the energy U_i of the impurity is independent of concentration. Suppose that a fraction $c_b(y)$ of the sites just outside the boundary are occupied by an impurity and that a frac-

tion $c_c(y)$ of the sites along the boundary are occupied. The Boltzmann factor $f_c=\exp(U_i/kT)$ favors the core sites. A given impurity atom selected for attention will divide its time between a bulk site and a core site in the ratio

$$(1-c_b):(1-c_c)f_c=c_b:c_c. \quad \text{(A2.1)}$$

This leads to

$$c_c=c_bf_c/[1+c_b(f_c-1)], \quad \text{(A2.2)}$$

which in turn leads to a ratio of concentration gradients along the core compared to the bulk given by

$$(\partial c_c/\partial y)/(\partial c_b/\partial y)=dc_c/dc_b = f_c/[1+c_b(f_c-1)]^2, \quad \text{(A2.3)}$$

the -1 in (f_c-1) being negligible for the cores of interest. Thus the "boost factor" f_c holds for low concentrations, but saturates when c_bf_c approaches unity. Since W_D is proportional to the ratio of diffusion current in the core to that in the bulk, W_D should vary as (A2.3). This leads to Eq. (31).

Equation (A2.3) neglects electrostatic interactions between donors along the core. These interactions will cause saturation effects to set in sooner by making U_i in effect a function of c_c.

In order to estimate the electrostatic effects, we note that the Debye length in silicon at 1200°C is given by

$$L_D=(\kappa kT/8\pi q^2n_i)^{\frac{1}{2}}=14 \text{ A}, \quad \text{(A2.4)}$$

where $\kappa=12$ is the dielectric constant and $n_i=2\times10^{19}$ cm^{-3}. L_D is about four times the spacing between sites at 1200°C. At 1050°C, L_D should be about 20 A. The electrostatic interaction between charges $b=3.83$ A apart is $q^2/\kappa b$, corresponding to an energy in electron volts of

$$300q/\kappa b=0.31 \text{ ev}. \quad \text{(A2.5)}$$

Since kT at 1200°C is about 0.126 ev, it is evident that electrostatic effects will become significant when about half the sites are occupied. This will not make major modifications in the form of Eq. (A2.3).

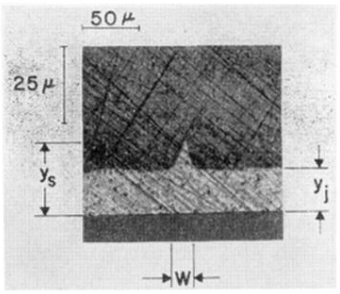

FIG. 3. Photograph of a beveled and stained *p-n* junction showing the diffusion front at the grain boundary.